THE ASTROPHYSICAL JOURNAL, 478:70–79, 1997 March 20

ORIGIN OF THE SPREAD IN THE $B-K$ COLOR OF QUASARS

R. SRIANAND AND AJIT KEMBHAVI
Inter-University Centre for Astronomy and Astrophysics, Post Bag 4, Ganeshkhind, Pune 411 007, India;
anand@iucaa.ernet.in, akk@iucaa.ernet.in
Received 1996 March 22; accepted 1996 October 15

ABSTRACT

Recently, Webster et al. have shown that there is excess reddening in radio-selected quasars relative to the optically selected population. If this reddening is universal to all quasars, then the optical surveys that depend on the UV-excess selection criteria, say, would be seriously incomplete. Using data compiled from the literature and various statistical tests, we show that there is no significant correlation between $B-K$ colors and other reddening indicators in the case of optically selected quasars. The distribution of emission-line equivalent widths and line ratios of radio-loud and radio-quiet quasars in the optically selected sample are consistent with their being drawn from the same parent population. Our results suggest that there is an intrinsic spread in $B-K$ color of ~ 2 mag in optically selected bright quasars due to effects other than dust.

Our model calculations suggest that the required amount of reddening cannot be produced by dust in the intervening damped Lyα absorbers. We estimate, for different extinction curves, the optical depth of dust intrinsic to quasars that is required to produce the observed spread in optical–to–near-IR colors. Results of photoionization models suggest that, for a wide range of ionization parameter and metallicity, the gas associated with dust will produce Lyman limit as well as saturated heavy-element absorption at the redshift of the quasar. Observation of such associated absorption in very red quasars will confirm reddening due to dust intrinsic to the quasar, but the data presently available suggest that the ~ 2 mag spread in $B-K$ color in the sample is due to effects other than dust extinction. We present marginal evidence for the aspect dependence of optical–to–near-IR colors in radio-loud quasars. This points to beaming as a possible reason for the reddening, but further investigation using a homogeneous sample is necessary before a conclusion can be reached.

Subject headings: galaxies: photometry — infrared: galaxies — quasars: general

1. INTRODUCTION

Recently, Webster et al. (1995) have shown that flat radio spectrum quasars, selected in the Parkes 2.7 GHz survey, have a much larger spread in $B-K$ color compared with optically selected bright quasars. From the absence of anti-correlation between $B-K$ color and rest equivalent width of the emission lines, Webster et al. argued that the emission-line region is exposed to a much harder continuum than that detected on Earth. They therefore ascribe the lack of very red optically selected quasars and the large spread in the $B-K$ of radio-selected objects to obscuration caused by line-of-sight dust. The inferred reddening is very high (extinction up to 5 mag in the B band) and, if true, will demand extensive revision in our knowledge of quasar astronomy.

Correlated continuum and emission-line variability studies confirm that the broad-line emission is due to the clouds' being photoionized by radiation from the central source. The observed equivalent widths of emission lines are remarkably constant over the full range of quasar luminosity. These imply a similar covering factor of the clouds and shape of the incident continuum in all quasars. However, Cheng, Gaskell, & Koratkar (1991) did not find any correlation between the equivalent width of Lyα + N v emission lines and UV spectral index, contrary to what is expected from the photoionization models. Thus the spectral energy distribution (SED) seen by the line-emitting clouds is different from what we observe, and the spread in the optical spectral index may be due to mild reddening.

If the observed spread in $B-K$ is not an intrinsic property of the quasars, it could be due to obscuration by dust located in regions close to the quasar itself. Some amount of reddening is always observed in low-redshift Seyfert galaxies. De Zotti & Gaskell (1985) have argued that since Seyfert galaxies and high-luminosity quasars have the same average Lyα-to-Hβ ratio, it would be remarkable if quasars were not reddened. Gaskell (1986) has also argued that the 2200 Å dust absorption feature is present in quasar spectra to the same degree as in UV spectra of Seyfert galaxies.

If the quasar is situated in a cluster of galaxies, the dust present in a member galaxy of the cluster that happens to lie along our line of sight can produce obscuration. This possibility is supported by the observations of Foltz et al. (1986). They have shown that radio-loud quasars tend to show associated C IV absorption lines more frequently than expected from randomly distributed absorbers. These associated absorbers are believed to be due to gas associated with galaxies in the cluster of which the quasar is also a member.

The obscuration could be due to dust in the host galaxy of the quasar, or in clouds (or in the intracloud medium) in the broad-line region (BLR), or in the narrow-line region (NLR) (Netzer & Laor 1993; Wills et al. 1993). Such a picture has been proposed to explain the observed asymmetry and relative shifts in the emission lines. The line reddening is also required to explain the observed hydrogen line ratios even after accounting for the high density and high optical depth conditions.

Another possible source of large $B-K$ color is the obscuration by dust located in the intervening galaxies or protogalaxies that happen to lie along our line of sight to quasars. Pei, Fall, & Bechtold (1991) have shown that

damped Lyα absorbers, which are presumed to be the progenitors of the present-day galaxies, along the line of sight to distant quasars do produce mild reddening.

Understanding the origin of the spread in $B-K$ is very important, as this could yield some vital clues toward understanding long-standing problems like (1) incompleteness in quasar number counts introduced by the optical selection techniques, (2) the fall in the spatial density of quasars at higher redshifts, (3) producing the amount of metagalactic ionizing UV background flux demanded by the deficit in the number density of Lyα absorption lines near quasars (the proximity effect), and (4) the origin of X-ray and IR background radiation.

Using a soft X-ray–selected sample of quasars, Boyle & di Matteo (1995) have demonstrated that the observed spread in the optical–to–X-ray flux ratio is consistent with an observed B-band extinction of less than $A_B \simeq 2$ mag. They have also argued that most of the spread could be due to effects other than dust obscuration and that the true upper limit to extinction is likely to be much lower. If their results are correct, then extinction in optical and UV spectra of quasars is very small. The observed spread in $B-K$ has to be explained as an intrinsic difference in the near-IR spectral shapes in the radio-loud and radio-quiet quasars. However, if the observed spread in $B-K$ is due to dust intrinsic to quasars, then the associated gas will also produce an appreciable amount of soft X-ray absorption, and the quasars can be missed in the soft X-ray surveys too.

In the framework of unification models for the radio-loud active galactic nuclei (AGNs), it is assumed that the torus is nearly face-on to our line of sight in the flat-spectrum radio sources (Antonucci 1993). Flat radio spectra in these objects are due to enhancement in the synchrotron emission from compact regions within a jet by relativistic beaming in the direction of motion. If such a beamed component exists in the optical emission as well, it could explain the unusually high $B-K$ colors of Parkes quasars (Serjeant & Rawlings 1996).

In this work, we try to understand the spread in the $B-K$ colors in the framework of the different possibilities discussed above. We have compiled an inhomogeneous data set from the literature and use it to obtain constraints on various alternatives. The details of the data set used in our analysis are given in § 2. We have looked for various correlations between the emission-line strengths and intensity ratios with the continuum spectral shapes. The results of the statistical analysis are discussed in § 3. In § 4, we describe the intrinsic spectral energy distribution used in our analysis. In § 5, we discuss a more realistic model for dust in the intervening damped Lyα systems and its contribution to the spread in the optical–to–near-IR colors. We discuss the effect of dust intrinsic to the quasar and its implications in § 6, and the results of our analysis in § 7.

2. DATA

We have compiled a list of all quasars from the literature for which near-IR photometry is available. The list includes quasars discovered using different selection methods, and our aim is to make a statistical comparison of their properties. The compilation includes the following: (1) The complete magnitude-limited, optically selected sample of bright quasars from Schmidt & Green (1983) (the Palomar-Green [PG] sample). The PG survey is complete to an average limiting magnitude of $B = 16.2$, and the 92 quasars in it are bluer than $U-B = -0.44$. Neugebauer et al. (1987) have obtained the SED for all these quasars from optical to near-IR wavelengths. (2) A sample of 30 serendipitous hard X-ray quasars (selected with follow-up optical identification complete up to 18.5 mag) with near-IR photometry by Neugebauer et al. (1982). Since these quasars are X-ray selected, they are free from bias due to dust. (3) Quasars from the Parkes flat-spectrum radio surveys with near-IR photometry by Glass (1981), Neugebauer et al. (1979), Hyland & Allen (1982), and Wright, Ables, & Allen (1983). (4) A sample of 14 radio-selected quasars and seven optical quasars with redshifts ($z \geq 2.6$) and near-IR photometry by Soifer et al. (1983).

We have added a few more quasars to the above sample from Capps, Sitko, & Stein (1982) and Impey & Brand (1981). Though our sample is inhomogeneous, as the data were originally drawn using different modes of selection, most of the quasars in it were discovered either in radio or in X-ray surveys, which are insensitive to the presence of dust. Thus the optical–to–near-IR colors of the sample are fairly unbiased toward dust extinction. In all, we have optical–to–near-IR colors for 263 quasars with $0 < z < 3$.

Boroson & Green (1992) have obtained strengths and equivalent widths of emission lines for all the PG quasars with $z \leq 0.5$. As the data were compiled by a single group and the spectral reduction procedure used for all these spectra are the same, the equivalent widths and line intensities are free from any bias due to extraction procedure and different signal-to-noise ratios in the spectra. We use this data for our correlation analysis in the following section.

3. EMISSION-LINE STRENGTHS AND CONTINUUM COLORS

We know that emission-line clouds are photoionized by radiation from the central continuum source. The equivalent widths of emission lines depend mainly on the slope of the continuum incident on the clouds. Extinction along the line of sight will alter only line ratios and will not change equivalent widths. Thus, studying the correlations between continuum slopes and the equivalent widths and line ratios will help in understanding the origin of the observed continuum slopes (i.e., whether these are intrinsic or reddened because of line-of-sight dust).

3.1. *Statistical Correlations*

We have looked for various possible correlations between emission-line equivalent widths and different colors and spectral indices for the PG quasar sample, *which is homogeneous in these data.* The results of nonparametric Spearman rank correlation tests are given in Table 1. Consistent with earlier results, we do not find any significant correlation between $B-K$ colors and equivalent widths of Hβ, O III, and He II emission lines. The null hypothesis that the observed correlation between two quantities arises by chance is significant at the $\sim 50\%$ level.

Barvainis (1990) has shown that the IR continuum in radio-quiet quasars can be explained as a combination of two purely thermal components. One component is due to warm dust in the inner kiloparsec or so of the host galaxy's nucleus that has been heated directly by the intense optical/UV continuum from the quasar. The second component, important in relatively low-luminosity objects, is thermal emission from stars and cool dust in the host galaxy's disk. If indeed the near-IR radiation is due to thermal emission from the hot dust in the torus, then one need not expect any

TABLE 1

RESULTS OF SPEARMAN RANK CORRELATION TEST

Variables	N	ρ	σ	ρ/σ	P
W(Hβ), $B-K$	73	0.103	0.118	0.872	0.3870
W(Hβ), α_{OX}	53	−0.494	0.139	−3.576	0.0002
W(Hβ), α_{op}	71	0.150	0.119	1.258	0.2110
W(O III), $B-K$	69	−0.101	0.121	−0.836	0.4080
W(O III), α_{OX}	51	−0.403	0.141	−2.850	0.0030
W(O III), α_{op}	68	−0.254	0.122	−2.080	0.0360
W(He II), $B-K$	57	−0.078	0.134	−0.580	0.5670
W(He II), α_{OX}	42	−0.166	0.156	−1.060	0.2940
W(He II), α_{op}	42	−0.256	0.135	−1.898	0.0570
Hα/Hβ, $B-K$	42	0.213	0.156	1.363	0.1760
Hα/Hβ, $B-H$	35	0.221	0.156	1.417	0.1590
Hα/Hβ, $B-J$	41	0.240	0.156	1.538	0.1250
Hα/Hβ, α_{OX}	31	−0.261	0.156	−1.676	0.0940
Hα/Hβ, α_{op}	31	0.058	0.156	0.373	0.7141
Hγ/Hβ, $B-K$	31	0.245	0.182	1.345	0.1820
Hγ/Hβ, $B-H$	31	0.278	0.182	1.525	0.1290
Hγ/Hβ, $B-J$	31	0.308	0.182	1.690	0.0910
Hγ/Hβ, α_{OX}	31	0.009	0.180	0.051	0.9607
Hγ/Hβ, α_{op}	31	−0.112	0.182	−0.617	0.5468

NOTE.—N is the number of quasars used, ρ is the correlation coefficient, σ is the standard deviation in ρ, and P is the probability that the two quantities are uncorrelated.

correlation between $B-K$ color and the equivalent width of emission lines for the quasars with $z < 0.5$. The lack of correlation found above is therefore not necessarily an indicator of the presence of line-of-sight dust.

We do not find any correlation between optical spectral index, α_{op}, and the equivalent width of Hβ. However, O III and He II emission-line equivalent widths show a weak 2 σ anticorrelation (see Boroson & Green 1992). The probability for the anticorrelation between two quantities to arise by chance is less than 5%, consistent with the predictions of simple photoionization models. We also find a significant anticorrelation between the Hβ and O III emission-line equivalent widths and X-ray–to–optical spectral index, α_{OX}. These results are consistent with the findings of Blumenthal, Keel, & Miller (1982) and Boroson & Green (1992).

We have also looked for possible correlation between the Balmer line intensity ratios and various colors and spectral indices. If the spread in the colors, or spectral shapes, is due to dust, then one would expect the Balmer line ratios to be correlated with the redness of the continuum. From Table 1, we do not find any significant correlation between intensity ratios of Balmer lines and continuum colors $B-K$, $B-H$, and $B-J$, α_{op}, and α_{OX}. It is known (Baldwin 1977) that Balmer line ratios in active galaxies are not consistent with what is expected from case B recombination, and Balmer decrements do not follow case B even if reddening is taken into account.

Our analysis therefore suggests that the spread in $B-K$ color seen in the optically selected sample is consistent with a nondust origin.

3.2. *Radio-loud and Radio-quiet Quasars*

The hypothesis of Webster et al. (1995) requires that the intrinsic properties of emission lines and colors of radio-loud and radio-quiet quasars be similar. We do not have a sufficiently large, homogeneous database of these properties to make a detailed comparison of the two kinds of objects. But we can examine the PG sample to see whether the properties of radio-loud and radio-quiet quasars in it are consistent with their being drawn from the same parent population.

Results of the two-parameter Kolmogorov-Smirnov (K-S) test applied to the two components in the PG sample are given in Table 2. As can be seen, the distribution of equivalent widths and continuum slopes of radio-loud and radio-quiet quasars in the sample are indeed consistent with their being drawn from a single population. However, it must be noted that, despite their name, radio-loud PG quasars in fact tend to have significantly lower 5 GHz luminosity and radio-to-optical luminosity ratios than radio-selected quasars and need not be representative of the radio-selected quasar population.

Earlier studies have shown that the optical spectra of radio-loud and radio-quiet quasars are remarkably similar. Neither Steidel & Sargent (1991) nor Corbin (1992) found any compelling spectral difference in higher redshift quasars. Francis, Hooper, & Impey (1993) have confirmed this result on the basis of composite spectra of radio-loud and radio-quiet quasars compiled from the Large Bright Quasar Survey (LBQS). However, they noted that at shorter wavelengths radio-loud quasars have narrower, higher equivalent width Lyα and C IV emission lines. These results imply that clouds in the BLR in radio-loud and radio-quiet quasars see similar radiation from the central source. However, the results quoted here are for bright quasars and are heavily biased against dust.

3.3. *Relativistic Beaming*

Using spectroscopic observations of 46 radio-loud quasars, Jackson et al. (1987) have shown that the equivalent width of the O III narrow emission line is strongly anticorrelated with the degree of radio core prominence. This provides evidence of an additional contribution to the optical emission in the case of core-dominated quasars. The excess emission can be attributed to relativistic beaming, which boosts the emission from a region with relativistic bulk motion at a small angle to the line of sight. If the beaming extends to the near-infrared as well, differences in the proportion of beamed radiation contributing to the two bands can lead to large $B-K$ colors.

In a simple beaming model (Orr & Browne 1982; Kembhavi 1993), the beamed luminosity can be written as

$$L^b(\theta) = \tfrac{1}{2} L_t^b [(1 - \beta \cos \theta)^{-(2+\alpha)} + (1 + \beta \cos \theta)^{-(2+\alpha)}] .$$

Here L_t^b is the intrinsic luminosity of the beamed part, i.e., the luminosity perceived when the beaming direction is perpendicular to the line of sight, θ is the viewing angle, and α is

TABLE 2

COMPARISON OF RADIO-LOUD AND RADIO-QUIET SAMPLES: RESULTS OF K-S TEST

Test Variable	N_1	N_2	D	$P(D)$
W(Hβ)	51	21	0.303	0.131
W(O III)	48	20	0.358	0.053
W(He II)	41	15	0.210	0.763
$B-K$	51	21	0.162	0.827
α_{OX}	33	19	0.185	0.804
α_{op}	49	21	0.265	0.252

NOTE.—D is the maximum difference between two cumulative distributions, and $P(D)$ is the probability of this maximum to occur by chance. N_1 and N_2 are the sizes of the subsamples.

the spectral index of the beamed emission. The excess in $B-K$ color due to beaming will depend on the luminosities $L_t^b(B)$ and $L_t^b(K)$ and spectral indices α_B and α_K. A right combination of these four parameters will produce the required excess in $B-K$ for a given viewing angle. However, the equivalent width of any optical emission line will depend only on $L_t^b(B)$ and α_B. In principle, therefore, one can produce large values of $B-K$ colors with very small variation in the equivalent widths by resorting to beaming. Beaming therefore does not require an obvious relation between equivalent width and $B-K$ color, despite the correlation mentioned at the beginning of this subsection. Thus the absence of correlation between $B-K$ colors and equivalent widths as noted by Webster et al. need not be a proof against reddening due to relativistic beaming.

In the following sections we will attempt to make some progress by modeling the line-of-sight dust in the different scenarios mentioned in § 1. We will discuss various implications of the estimated dust optical depth needed in different models to produce the observed reddening and make a comparison with available observations. Our attempt will be to see whether any of the scenarios lead to plausible models. Before we do the dust modeling, in the following section we discuss the intrinsic SED of our model quasar.

4. INTRINSIC SPECTRAL ENERGY DISTRIBUTION

It is important to specify the intrinsic spectrum of a typical quasar before going into the details of various models. Most of the studies in the literature assume the shape of the quasar continuum to be a simple power law. Since quasars have strong emission lines and different components of the continuum emission (like the big blue bump and Balmer continuum), one should use a more realistic spectrum than a simple power law, as different features will contribute to the observed colors at different redshifts.

Francis et al. (1991) have compiled a composite spectrum using the spectra of 718 quasars from the LBQS. This spectrum has been shown to represent the average radio-loud quasars too (Francis et al. 1993). Thus it will be a good approximation to assume this to be the typical UV-to-optical spectral energy distribution for all quasars. In what follows we use this composite spectrum as the unreddened intrinsic quasar spectrum. This covers the rest wavelength range between 800 and 6000 Å. We have extrapolated the Francis et al. (1991) composite up to 1 μm and added the Hα emission line, with equivalent width 300 Å.

It is believed that most of the near-IR emission from the quasar is due to dust heated by the central source. The near-IR bump starts around 1–2 μm and will affect the K band only for low redshifts (say, $z \lesssim 0.4$). We have assumed the SED in the near-IR to be a power law with spectral index between 0.5 and 2.0 to allow for the uncertainties in the IR spectral shape. This range is necessary to cover the observed IR colors $J-K$ and $H-K$ in the low-redshift quasars in our sample. It may be noted here that in order to explain the observed near-IR colors of PG quasars, the nonthermal emission needs to have power-law indices in the range 1.0–2.2 (Berriman 1990).

Another component of the SED of quasars, which is important in relatively low luminosity objects, is the stellar continuum emission from the host galaxy. Using the SED of radio-quiet AGNs, Kriss (1988) has determined that the fraction of the continuum at 1 μm contributed by stellar light from the host galaxy is $\lesssim 7.5\%$, using a sample of radio-quiet quasars with X-ray luminosity at 2 keV greater than 6×10^{24} ergs s^{-1} Hz^{-1}. Using the PG sample, Neugebauer et al. (1989) have shown that the host galaxy can contribute as much as 40% of the total measured flux, but the typical value is $\sim 10\%$. Using near-IR colors of elliptical galaxies, Berriman (1990) has shown that even though starlight becomes much redder with redshift as a result of K-correction, it only becomes as red as quasars in the small redshift interval 0.35–0.4. We have decided to ignore this component, as it will not contribute appreciably to the observed colors of quasars over a wide range of redshifts. However, we note that the host galaxy contribution may be important in the case of some of the faint sources in our sample.

In Figure 1, we have plotted the different observed colors of quasars in our sample against their redshifts. Also shown are the colors obtained by passing a suitably redshifted input spectrum through filters with standard response functions, with zero-point calibrations obtained from Neugebauer et al. (1987) and Zombeck (1990, p. 100). The predicted curves cover most of the observed $B-K$ range at low redshift but underestimate the width of the distribution at higher redshifts. We do not find many quasars below the predicted lines. Thus a simple unreddened model cannot explain the spread in $B-K$ for $z \geq 0.3$. The dip seen in the $H-K$ colors between $z = 1.2$ and $z = 1.8$ is produced by the excess flux due to Hα emission lines.

5. THE EFFECT OF DUST IN DAMPED Lyα ABSORBERS

The effect of intergalactic dust on observations of objects at cosmological distances has been discussed by Ostriker & Heisler (1984), Heisler & Ostriker (1988), and Wright (1986). These authors have shown that a small amount of dust along the line of sight to a high-redshift quasar can redden the quasar appreciably and remove it from a magnitude-limited sample. It is widely believed that damped Lyα absorbers at high redshifts are the progenitors of the present-day galaxies. Pei et al. (1991) have shown that quasars with damped Lyα systems along the line of sight are redder than those without such systems in the foreground. They interpret this as an effect of reddening due to a small amount of dust in the systems.

The presence of a small amount of dust in these absorbers has been confirmed by Pettini et al. (1994), using Zn^+ and Cr^+ absorption lines. In a recent study of the proximity effect, Srianand & Khare (1996) have shown that the ionization background calculated using quasars with damped Lyα absorption in the foreground is ~ 3 times less than the values obtained for the whole sample. This confirms the presence of dust in the absorbers. Thus the spread in the $B-K$ color can be due to obscuration by dust in the damped Lyα absorbers. In what follows we construct a realistic model of dust in these absorbers and estimate its contribution to the spread in $B-K$ color.

The average optical depth of dust along the line of sight at any redshift can be written as

$$\bar{\tau}(z) = \int_0^z dz' \int_0^\infty d\tau\, \tau \rho(\tau, z') \,, \qquad (1)$$

where $\rho(\tau, z) dz\, d\tau$ is the mean number of absorbers along the line of sight with optical depth between τ and $\tau + d\tau$ and redshift between z and $z + dz$. In the

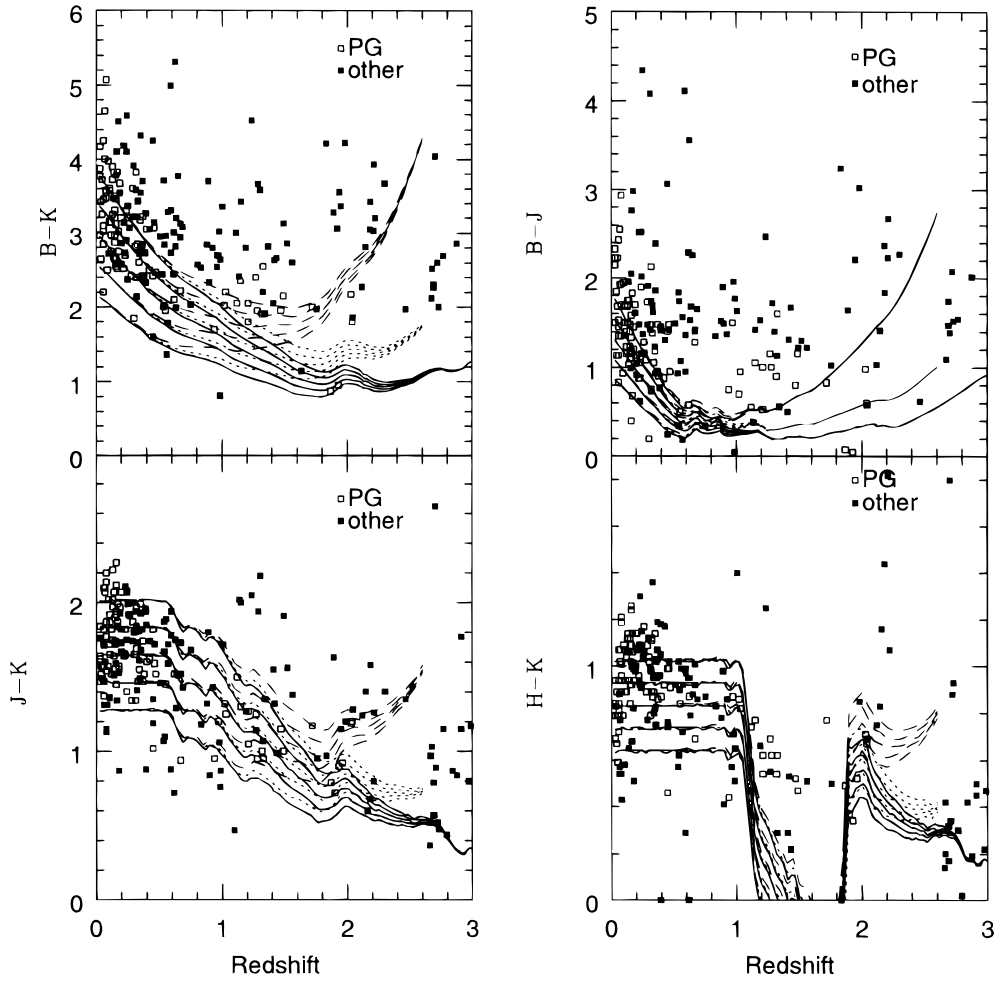

FIG. 1.—Effect of damped Lyα absorbers on quasar colors. The curves are predicted distributions for different models of reddening due to intervening damped Lyα clouds. The solid, short-dashed, and long-dashed curves represent the results for no reddening, low reddening, and maximum reddening models, respectively. Open squares are data points for PG quasars, and filled squares represent other quasars in our sample.

Friedmann universe,

$$\rho(\tau, z)d\tau = (1 + z)\sqrt{1 + 2q_0 z}\, f(N, z)dN\ , \qquad (2)$$

where $f(N, z)$ is the mean number of absorbers along a random line of sight with H I column density between N and $N + dN$ and redshift in the range from z to $z + dz$. The optical depth in the rest frame of the observer at $z = 0$ is related to the column density of the absorber by

$$\tau = \left[\frac{k(z)N}{10^{21}\ \mathrm{cm}^{-2}}\right]\xi\left(\frac{\lambda_B}{1 + z}\right), \qquad (3)$$

where $\xi(\lambda)$ is the ratio of the extinction at a wavelength λ to that in the B band and k is the dimensionless dust-to-gas ratio.

Using equations (1), (2), and (3), one can write

$$\bar{\tau}(z) = (104\ h)\int_0^z dz'\,\frac{k(z')\Omega_{\mathrm{H\,I}}(z')(1 + z')}{\sqrt{1 + 2q_0 z'}}\,\xi\left(\frac{\lambda_B}{1 + z'}\right), \qquad (4)$$

where h is Hubble's constant in units of 100 km s^{-1} Mpc^{-1} and

$$\Omega_{\mathrm{H\,I}}(z) = \frac{8\pi G m_{\mathrm{H}}}{3cH_0}\int_0^\infty dN\, N f(N, z) \qquad (5)$$

is the mean comoving density of H I in damped Lyα systems, in units of the present critical density, defined in terms of the column density distribution of neutral hydrogen.

The observed flux, $f_o(\lambda_o)$, and the emitted flux, $f_e(\lambda_e)$, are related by

$$f_o(\lambda_o) = \frac{f_e(\lambda_e)}{1 + z_e}\exp\left[-\int_0^{z_{\mathrm{em}}} dz_a\,\bar{\tau}_a\left(\frac{\lambda_o}{1 + z_a}\right)\right], \qquad (6)$$

where $\bar{\tau}_a$ is the mean optical depth of the intervening absorber at redshift z_a. Thus for a given extinction curve (or for a given grain composition), the effect of dust in the damped Lyα systems can be modeled with two parameters (k and $\Omega_{\mathrm{H\,I}}$).

We now need a prescription for the evolution of $\Omega_{\mathrm{H\,I}}(z)$. From the LBQS survey for damped Lyα absorbers, Wolfe et al. (1995) have shown that the evolution can be parameterized as

$$\Omega_{\mathrm{H\,I}}(z) = \Omega_{\mathrm{H\,I}}(0)\exp \alpha z\ , \qquad (7)$$

where $\Omega_{\mathrm{H\,I}}(0)$ is the density of neutral hydrogen gas at $z = 0$ and α is a constant characterizing the rate of evolution. For $q_0 = 0.5$, Wolfe et al. obtained $\Omega_{\mathrm{H\,I}}(0) = (0.23 \pm 0.08) \times 10^{-3}\ h^{-1}$ and $\alpha = 0.70 \pm 0.15$. For k we can use the value

$0.35^{+0.24}_{-0.09}$ obtained by Pei et al. (1991) for Galactic extinction curves. As noted by Fall & Pei (1993), $\Omega_{\rm H\,I}(z)$ calculated from damped Lyα in the foreground of optically selected quasars is probably biased by the very obscuration we wish to estimate, and the observed values of $\Omega_{\rm H\,I}$ and k may very well be lower limits. We therefore refer to a model in which these values for the parameters are used as a *low-reddening model.*

There is another way to obtain the parameters, using an upper limit on $\Omega_{\rm H\,I}$ from big bang nucleosynthesis calculations. Boesgaard & Steigman (1985) have estimated the baryon density Ω_b, based on nucleosynthesis, at 0.034–0.048. Steidel (1990) has estimated that at $z = 3$ the contribution of Lyman limit systems to the cosmological density is $\Omega_{\rm LLS} = 0.004$. The contribution of luminous matter is estimated to be $\Omega_{\rm lb} \simeq 0.002$ (Persic & Salucci 1992). The baryonic density in the intergalactic medium, $\Omega_{\rm IGM}$, can be estimated from the Gunn-Peterson effect to be less than 0.004 (Giallongo et al. 1994). One can then write

$$\Omega_b = \Omega_{\rm IGM} + \Omega_{\rm LLS} + \Omega_{\rm H\,I}^{\rm dLy\alpha} + \Omega_{\rm lb}\,, \tag{8}$$

and thus the maximum value of $\Omega_{\rm H\,I}$ that can be in the damped Lyα systems, $\Omega_{\rm H\,I}^{\rm dLy\alpha}$, at $z \simeq 3$ is 0.032.

Results from radio observations of nearby galaxies (Rao & Briggs 1993) have shown that there is not much bias in the values of $\Omega_{\rm H\,I}(0)$ obtained from low-z damped Lyα surveys. Using equation (7), assuming that it remains valid in the present case too, and using the maximum inferred $\Omega_{\rm H\,I}$ at $z = 3$ yields $\alpha \simeq 1$. We now define *maximum reddening models* as those with $\alpha = 1, \Omega_{\rm H\,I}(0) = 0.23 \times 10^{-3}\ h^{-1}$, given by Rao & Briggs (1993), and dust-to-gas ratio $k = 0.8$ as observed in our Galaxy.

In Figure 1, we show curves corresponding to the expected colors of model quasars, situated at different redshifts, for the two dust models. It is clear from the figure that, for the range of near-IR spectral indices, the models with no reddening yield a lower envelope of the $B-K$ color at all redshifts. Low as well as maximum reddening models fail to produce sufficient reddening at low redshifts as seen in the observed distribution. Note that our maximum extinction model assumes that all the unobserved baryons are in damped Lyα systems with maximum dust-to-gas ratio and still fails to produce the observed spread in the $B-K$ color at low redshift.

Thus our analysis clearly shows the observed spread at low z is not due to the reddening of quasars by the intervening objects. However, these models produce appreciable reddening at higher redshifts. Masci & Webster (1995) also reached similar conclusions, using the methods prescribed by Heisler & Ostriker (1988) to estimate the optical depth of intervening dust. The effect of dust in the damped Lyα clouds on, e.g., quasar counts, UV ionizing background radiation, and the "cosmic G-dwarf problem" are discussed in detail in Pei & Fall (1995).

6. EFFECT OF DUST INTRINSIC TO QUASARS

Dust can be present in the BLR and NLR of the quasars either inside clouds or in the intracloud medium. The extinction can also be caused by a dusty torus, or by dust in the host galaxy or cluster of galaxies of which the quasar is a member. In this section, we estimate the amount of dust needed to explain the spread in the $B-K$ colors in these scenarios.

Since we do not know the exact extinction curve for the associated dust, we have used mean extinction curves of our Galaxy, the LMC, and the SMC (Savage & Mathis 1979; Nandy et al. 1981; Pervot et al. 1984). We can write the optical depth of dust at different wavelengths in terms of optical depth in the B band, τ_B, as

$$\tau_\lambda = \tau_B\,\xi(\lambda); \tag{9}$$

τ_B can be obtained by comparing the predicted distribution of colors with the observed distribution. One can obtain the total hydrogen column density from τ_B by using equation (3) for an assumed dust-to-gas ratio. The estimated maximum B-band optical depth required to produce the upper envelope (i.e., on an average $B-K$ color of ~ 5.0 for all redshifts) of the observed color distribution, $\tau_B^{\rm max}$, and the total column density, $N_{\rm H}^{\rm total}$, for k similar to and one-tenth of the dust-to-gas ratio in the interstellar medium (ISM) of the Galaxy, LMC, and SMC are given in Table 3. The predicted distribution for different values of τ_B (0.0, 0.2, and 0.35 in the rest frame of the quasar) for a Galactic extinction curve are given in Figure 2.

6.1. *Dust in the BLR*

The obscuring dust can be present in the individual broad-line–emitting clouds. It is believed that the surface covering factor of clouds in the BLR is ~ 0.10. Thus only a few percent of the quasars will have a broad-line–emitting cloud along our line of sight. If the dust is indeed present in the broad-line clouds, the obscuration will be greater for the resonance lines, as the path lengths of these photons are large because of resonance capture. AGN observations do not show any large reduction in the strengths of resonance lines like Lyα and C IV compared with calculated intensity of the intercombination lines, like C III] λ1909. Therefore the amount of dust in the BLR clouds is unlikely to be significant.

From reverberation-mapping studies of the broad-line region in nearby AGNs, the radius of the BLR may be estimated to be $\sim 0.06 L_{46}^{0.5}$ pc (Netzer & Laor 1993), where L_{46} is the bolometric luminosity in units of 10^{46} ergs^{-1}. On the other hand, Laor & Draine (1993) have shown that the sublimation radius from the central engine at which even large graphite grains will sublimate is $\sim 0.2 L_{46}^{0.5}$ pc. Thus dust cannot survive inside the BLR, and the required reddening is not caused by the BLR clouds. It follows that any obscuring dust must be present outside the BLR.

6.2. *Dust and Associated Gas outside the BLR*

Dust outside the BLR may be present in the NLR, or in the host galaxy of the quasar, or in another galaxy in a cluster of which the quasar is a member. In all these cases, the dust must be present together with gas, the ionization

TABLE 3

PARAMETERS OF INTRINSIC DUST

		log $N_{\rm H}^{\rm total}$	
DUST MODEL	$\tau_B^{\rm max}$	Model A	Model B
Galactic.....	0.35	20.60	21.60
SMC	0.25	21.70	22.70
LMC	0.30	21.00	22.00

NOTE.—Model A and model B are, respectively, models with dust-to-gas ratio similar to and one-tenth that of the Galaxy, LMC, and SMC.

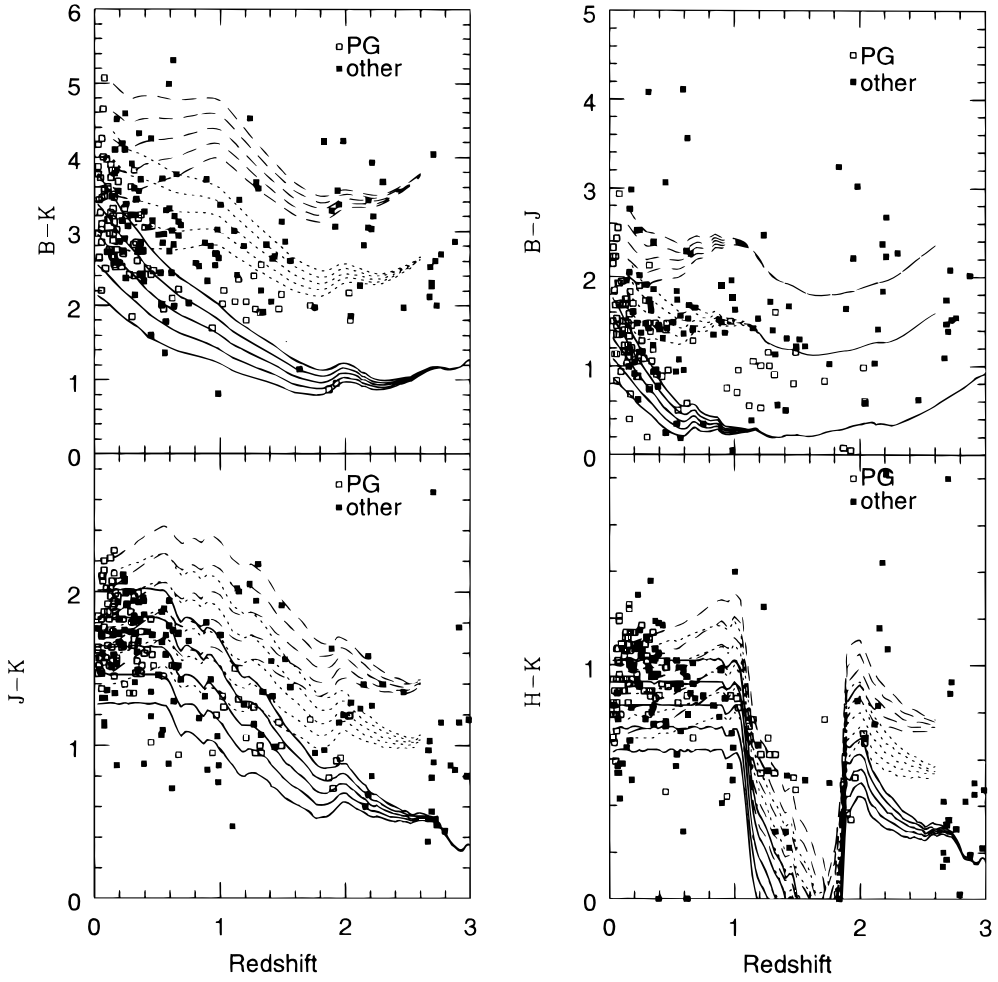

FIG. 2.—Effect of intrinsic dust on quasar colors. The curves are predicted distributions for different dust optical depths intrinsic to quasars for a Galactic extinction curve. The solid, short-dashed, and long-dashed curves are for dust optical depths of 0.0, 0.20, and 0.35, respectively. Open squares are data points for PG quasars, and filled squares represent other quasars in our sample.

structure of which is determined by the radiation from the quasar. So if the reddening in a quasar is due to dust in such locations, there should be signatures of the associated gas in the quasar spectra. We will now examine the ionization structure of gas associated with the dust and its implications, using photoionization models together with absorption-line data available in the literature.

We assume that the absorber is a plane-parallel slab with total hydrogen column density obtained using parameters for the Galactic extinction curve given in Table 3. We have constructed grids of photoionization models for a range of ionization parameters using the code CLOUDY (Ferland 1993). We have assumed that the metal abundances and dust-to-gas ratio are similar to (model A) and one-tenth of (model B) the average ISM values of our Galaxy (Cowie & Songaila 1986) and that the incident ionizing radiation has a typical AGN spectrum. We have assumed values of the ionization parameter to be in the range $-3.5 < \log \Gamma < -1.5$. This is the typical range used in photoionization calculations for absorption-line systems (Srianand & Khare 1994) and NLR clouds (Osterbrock 1989).

The resulting column densities of neutral hydrogen and different ionization states of several heavy elements are shown in Figure 3. When the ionization parameter $\log \Gamma < -2.5$, the neutral hydrogen is in the damped portion

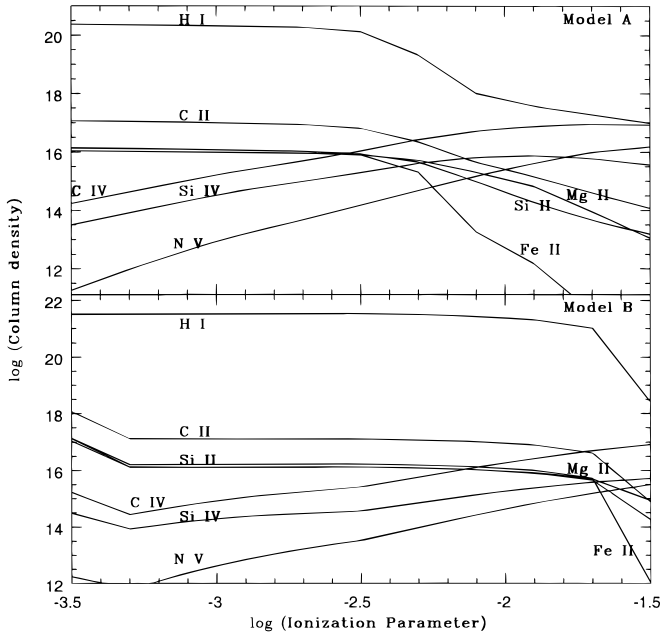

FIG. 3.—Results of photoionization calculations for dust-to-gas ratio similar to (model A) and one-tenth that of mean value of the Galactic ISM.

of the curve of growth. In the case of low metallicity, the neutral hydrogen will be damped almost over the whole range of ionization parameter considered here. This will produce damped Lyα absorption on top of the Lyα emission lines. However, there is no example of damped Lyα at the redshift of the quasar itself in the available data. This clearly rules out the absorber's producing reddening from having an ionization structure similar to that in our Galaxy (i.e., with the column density of H I almost equal to the total hydrogen column density).

Even if the ionization parameter and metallicity are high, the neutral hydrogen optical depth at the Lyman limit is high and the associated gas will produce the Lyman limit break at the emission redshift. Note that the total hydrogen column densities inferred for LMC and SMC extinction curves are higher than that obtained using the Galactic extinction curve. Models using dust-to-gas ratios similar to those in the LMC and SMC will therefore produce a higher neutral hydrogen optical depth for the same range of Γ.

Koratkar, Kinney, & Bohlin (1992) have searched for associated Lyman limit absorption (i.e., the Lyman limit break with $z_{\rm abs} \simeq z_{\rm em}$) and detected this in 12% of the cases. If the large values of $B-K$ are due to extinction caused by these absorbers, then one should expect the red objects to show associated Lyman limit absorption. We have looked for such an effect in the quasars for which Lyman limit observations (from Bahcall et al. 1993; Lanzetta, Wolfe, & Turnshek 1995; Koratkar et al. 1992) as well as $B-K$ colors are available. We define an absorption system to be an associate system of a quasar when its relative velocity with respect to the quasar is less than 500 km s^{-1}. The relative velocity is defined as

$$v = \frac{c\,\Delta(z)}{1+\bar{z}}\,, \tag{10}$$

where z_a is the redshift of the absorption system, $\Delta(z) = z_e - z_a$, and $\bar{z}$ is $(z_e + z_a)/2$. In Figure 4*a* we have plotted

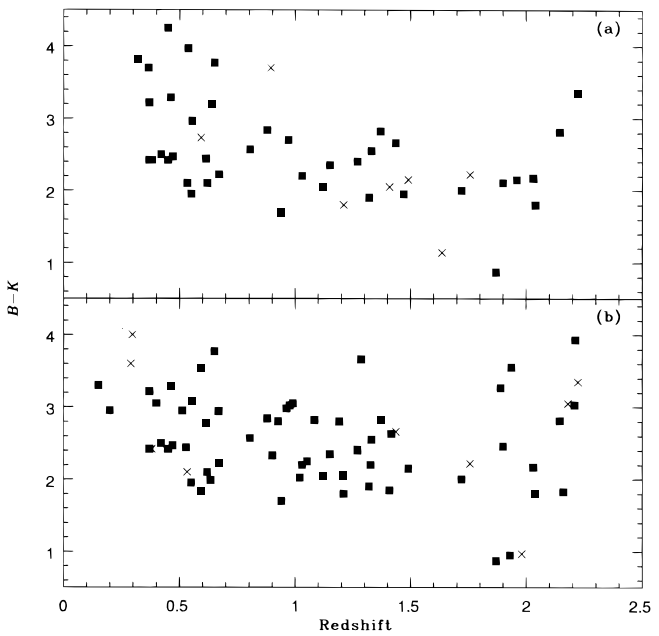

FIG. 4.—$B-K$ color as a function of redshift for the quasars that are studied for the presence of associated (*a*) Lyman limit and (*b*) metal-line absorption.

$B-K$ color as a function of redshift for this subsample. We denote the quasars with an associated Lyman limit discontinuity with crosses. It is clear from this figure that there is no tendency for red quasars to show associated absorption. However, note that since low-redshift Lyman limit data are compiled using satellite-based telescopes, they are available only for bright objects and are biased against reddening.

Another interesting point to note in Figure 3 is that almost all the ions have column densities greater than 10^{14} cm^{-2} for the range of ionization parameter considered here. This is also true for the models with dust-to-gas ratio similar to the LMC and SMC, as the total hydrogen column density is high. This will imply strong saturated absorption lines on top of all the emission lines. Thus one should see associated heavy-element absorption lines preferentially in red quasars. We have collected the absorption-line (mainly Mg II absorption lines in the redshift range 0.3–2.2) data for 75 quasars in our sample (Steidel & Sargent 1992; Lanzetta, Turnshek, & Wolfe 1987; Aldcroft, Bechtold, & Elvis 1994). In Figure 4*b* we have plotted $B-K$ color as a function of redshift for the quasars with absorption-line information. In this figure, we denote quasars with associated heavy-element systems with crosses. It is clear from the figure that there is no tendency for red quasars to show excess associated absorption.

In order to produce $B-K \geq 3$, one needs $\tau_B > 0.25$ if the unreddened spectrum is similar to the composite of Francis et al. (1991). For a dust-to-gas ratio similar to the Galactic ISM, this will correspond to a total hydrogen column density of less than 3×10^{20} cm^{-2}. Photoionization models of such a cloud predict the column density of C IV and Mg II to be greater than 10^{14} cm^{-2} for a wide range of parameters. This will mean strong saturated absorption. If the intrinsic spectrum of all quasars is similar to the SED of optically selected quasars, then all quasars with $B-K > 3.0$ should show associated intrinsic absorption. There are 18 quasars with $B-K > 3$ for which good-quality absorption-line spectra are available in our sample, of which only four show associated absorption. Using 5 σ upper limits on the equivalent widths of Mg II (0.3 Å) and C IV (0.15 Å) absorption lines for these quasars, we estimate an upper limit on dust optical depth of $\tau_B < 10^{-3}$. Thus our results suggest that the intrinsic spread in the $B-K$ color of 2 mag seen in our sample is produced by effects other than reddening. Note that our sample does not have very red quasars (i.e., with $B-K > 5.0$) as in the case of the Webster et al. sample. The presence (or absence) of associated absorption in these quasars will favor the dust models and can provide a tight bound on the dust optical depth.

Evidence for extinction due to dust in the associated absorbers is available for just a few cases in the literature. Sprayberry & Foltz (1992) have inferred a small amount of dust extinction in the case of low-ionization broad absorption line quasars (BALs). However, it is known that BALs are rare among radio-loud quasars. Thus the red continua in the Parkes quasars cannot in general be due to dust in BAL gas. Using X-ray and UV data, Mathur (1994) and Mathur et al. (1994) have shown that in the case of the red quasars 3C 212 and 3C 351 an associated warm absorber is responsible for both soft X-ray and UV absorption. However, the nondetection of associated absorbers preferentially in the red objects, as reported here, suggests that the dust intrinsic to the quasar is not the main contributor to the 2 mag spread in the $B-K$ color of the quasars in our sample.

7. DISCUSSION

The various results discussed above suggest that the spread in $B-K$ color of quasars up to ~ 2 mag is caused by effects other than reddening due to line-of-sight dust. There are several possible explanations for the observed large spread in $B-K$ colors.

As part of a survey of quasar continuum spectra, McDowell et al. (1989) identified a class of quasars in which the optical/ultraviolet continuum "blue bump" feature appears to be weak or absent relative to both IR and soft X-rays. They showed this suppression to be due to effects other than dust extinction. These quasars are normal objects apart from a weak "blue bump." They also tend to have large $B-K$ colors and are easily detectable in radio surveys. If most of the red quasars in the sample of Webster et al. (1995) are weak blue bump quasars, then optical surveys will miss a large fraction of them. However, these quasars have soft X-ray properties similar to those of normal quasars, and soft X-ray surveys should pick up more of such objects. Clearly, the observations of Boyle & di Matteo (1995) rule out this possibility.

Another possible alternative is that most of the observed spread in $B-K$ in flat-spectrum quasars is due to some property peculiar to those objects. In unified models of radio-loud AGNs, it is believed that the torus is nearly perpendicular to the line of sight in the case of flat radio spectrum sources. The flat spectrum is believed to be due to self-absorbed synchrotron emission that is boosted as a result of relativistic bulk motion of the compact emitting regions. The large values of $B-K$ in quasars selected in the flat-spectrum surveys could also be due to a beamed component at near-IR wavelengths. In order to check this possibility, we have searched for the value of R (defined as the ratio of radio core flux density to the extended radio lobe flux density) for quasars in our sample in the literature and obtained it in most cases from Wills & Browne (1986), Browne & Murphy (1987), and Wills et al. (1992). In the relativistic beaming model for radio sources, R is related to the angle between the radio axis and the line of sight. In Figure 5, we have plotted different colors of quasars in the sample against R. It can be seen from the figure that, on average, the core-dominated quasars tend to be redder than the lobe-dominated quasars. We have performed the Spearman rank correlation test between log R and different optical–to–near-IR colors, and the results are given in Table 4. These results suggest a weak correlation between the optical–to–near-IR colors of the quasars and log R, despite the large spread shown in Figure 5.

Using composite spectra of the Molonglo sample of quasars, Baker & Hunstead (1995) have shown that reddening is considerable in most lobe-dominated quasars. They have also shown the extinction to be aspect dependent, with the reddening decreasing with R, which is in the sense opposite to what is found in our analysis. Their sample was originally selected at 408 MHz, where steep-spectrum extended emission dominates. The typical value of log R in the lobe-dominated quasars is between -2 and -1 (Orr & Browne 1982). In order to compare Baker & Hunstead's results with ours, we have split our data into two subsamples, with log $R > -1$ and log $R < 0$, respectively, and performed Spearman rank correlation tests separately on the subsamples. The results of these tests are also given in Table 4. It is clear from the table that if we consider only quasars with log $R > -1$ (i.e., consider only marginally lobe-dominated and core-dominated quasars) the correlation between log R and optical–to–near-IR color increases and becomes more significant. When we consider only lobe-dominated quasars (i.e., quasars with log $R < 0$), we find significant anticorrelation between log R and optical–to–near-IR colors, consistent with the finding of Baker & Hunstead (1995). Thus our results suggest that, consistent with simple unification models of radio-loud AGNs, both extremely lobe-dominated and extremely core-dominated quasars tend to be red. While obscuration is the cause in the case of lobe-dominated quasars, in core-dominated quasars nonthermal beamed emission may be the source of the reddening. Antonucci (1993) has also shown from the studies of steep-spectrum radio sources that narrow-line radio galaxies are in fact obscured quasars. Note that our sample is drawn from different sources in the literature and is affected by unknown selection biases. Our data set also does not have the very red quasars that are

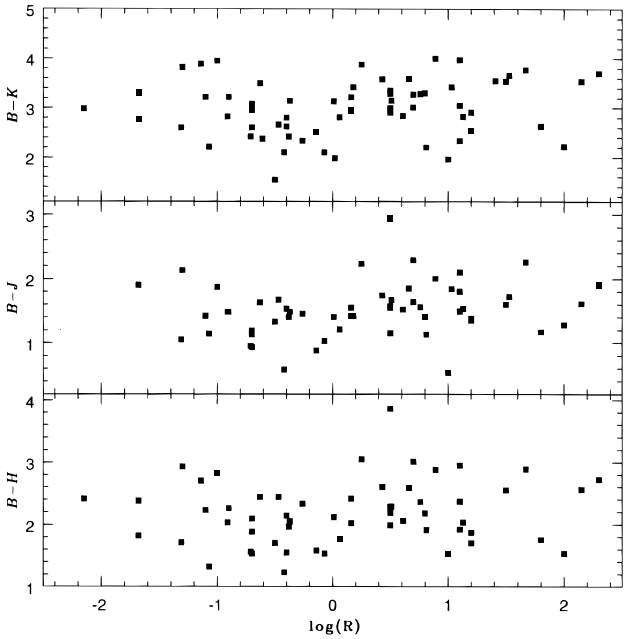

FIG. 5.—Quasar colors as a function of R, defined as the ratio of radio core flux density to the extended radio lobe flux density.

TABLE 4

CORRELATION BETWEEN log R AND OPTICAL–TO–NEAR-IR COLORS

Variables	N	ρ	σ	ρ/σ	P
log R, $B-K$.....	66	0.23	0.13	1.85	0.064
log R, $B-J$	58	0.29	0.13	2.17	0.028
log R, $B-H$.....	59	0.17	0.13	1.30	0.198
log $R > -1$					
log R, $B-K$.....	57	0.38	0.13	2.86	0.003
log R, $B-J$	52	0.40	0.14	2.83	0.004
log R, $B-H$.....	50	0.29	0.14	2.06	0.040
log $R < 0$					
log R, $B-K$.....	27	−0.52	0.20	−2.64	0.003
log R, $B-J$	22	−0.32	0.22	−1.49	0.014
log R, $B-H$.....	26	−0.35	0.20	−1.75	0.199

NOTE.—N is the number of quasars used, ρ is the correlation coefficient, σ is the standard deviation in ρ, and P is the probability that the two quantities are uncorrelated.

present in the Webster et al. (1995) sample. Confirming the trend noted here with a complete radio-selected sample like the one used by Webster et al. will favor beaming models.

Since the Webster et al. (1995) sample predominantly consists of core-dominated quasars (Parkes sample), the observed reddening could be due to relativistic beaming. If the beaming extended up to X-ray energies, then one would expect to see the total X-ray luminosity, L_X, to increase with total radio luminosity, L_r, in the beamed quasars (Kembhavi 1993). Thus, observing a flat X-ray spectrum and low equivalent widths predominantly in the quasars with large $B-K$, in a homogeneous sample, will strengthen the beaming hypothesis.

In conclusion, we have shown that the observed redness of the quasars cannot be due to dust in the intervening damped Lyα clouds. We have argued that the dust cannot survive in the BLR region, either inside or outside the clouds. We have shown, using photoionization models, that if the reddening is caused by dust associated with the quasar, the gas associated with the dust will produce heavy-element absorption lines and a Lyman limit break at the emission redshift of the quasars. Finding associated heavy-element absorption in very red quasars will support the dust models. One can place stringent constraints on the dust optical depth from the properties of the associated absorption lines. Our analysis suggests that highly core-dominated and highly lobe-dominated quasars tend to be red. Observing very large values of R for quasars with high $B-K$ and with no associated absorption lines will confirm the beaming model.

We wish to thank Professor Gary Ferland for his help throughout the course of this work. We would like to thank an anonymous referee for his useful comments, which helped to improve this paper considerably.

REFERENCES

Aldcroft, T. L., Bechtold, J., & Elvis, M. 1994, ApJ, 93, 1
Antonucci, R. 1993, ARA&A, 31, 473
Bahcall, J. N., et al. 1993, ApJS, 87, 1
Baker, J., & Hunstead, R. W. 1995, ApJ, 452, L95
Baldwin, J. A. 1977, MNRAS, 178, 67P
Barvainis, R. 1990, ApJ, 353, 419
Berriman, G. 1990, ApJ, 354, 148
Blumenthal, G. R., Keel, W. C., & Miller, J. S. 1982, ApJ, 257, 499
Boesgaard, A. M., & Steigman, G. 1985, ARA&A, 23, 319
Boroson, T. A., & Green, R. F. 1992, ApJS, 80, 109
Boyle, B. J., & di Matteo, T. 1995, MNRAS, 277, L63
Browne, I. W. A., & Murphy, D. W. 1987, MNRAS, 226, 601
Capps, R. W., Sitko, M. L., & Stein, N. A. 1982, ApJ, 255, 413
Cheng, F. H., Gaskell, C. M., & Koratkar, A. P. 1991, ApJ, 370, 487
Corbin, M. R. 1992, ApJ, 391, 577
Cowie, L. L., & Songaila, A. 1986, ARA&A, 24, 499
De Zotti, G., & Gaskell, C. M. 1985, A&A, 147, 1
Fall, S. M., & Pei, Y. C. 1993, ApJ, 402, 479
Ferland, G. J. 1993, HAZY, a Brief Introduction to Cloudy (Univ. Kentucky Phys. and Astron. Dept. Internal Rep.)
Foltz, C. B., Weymann, R. J., Peterson, B. M., Sun, L., Malkan, M. N., & Chaffee, F. H., Jr. 1986, ApJ, 307, 504
Francis, P. J., Hewett, P. C., Foltz, C. B., Chaffee, F. H., Weymann, R. J., & Morris, S. L. 1991, ApJ, 373, 465
Francis, P. J., Hooper, E. J., & Impey, C. D. 1993, AJ, 106, 417
Gaskell, C. M. 1986, in Continuum Emission in Active Galactic Nuclei, ed. M. L. Sitko (Tucson, AZ: NOAO), 39
Giallongo, E., D'Odorico, S., Fontana, S., McMahon, R. G., Savaglio, S., Cristiani, S., Molaro, P., & Trevese, D. 1994, ApJ, 425, L1
Glass, L. S. 1981, MNRAS, 194, 795
Heisler, J., & Ostriker, J. P. 1988, ApJ, 332, 543
Hyland, A. R., & Allen, D. A. 1982, MNRAS, 199, 943
Impey, C. D., & Brand, P. W. J. L. 1981, Nature, 292, 814
Jackson, N., Browne, I. W. A., Murphy, D. W., & Saikia, D. J. 1987, Nature, 338, 485
Kembhavi, A. 1993, MNRAS, 264, 683
Koratkar, A. P., Kinney, A. L., & Bohlin, R. C. 1992, ApJ, 400, 435
Kriss, G. A. 1988, ApJ, 324, 809
Lanzetta, K. M., Turnshek, D. A., & Wolfe, A. M. 1987, ApJ, 322, 739
Lanzetta, K. M., Wolfe, A. M., & Turnshek, D. A. 1995, ApJ, 440, 435
Laor, A., & Draine, B. T. 1993, ApJ, 402, 441
Masci, F. J., & Webster, R. L. 1995, Publ. Astron. Soc. Australia, 12, 146
Mathur, S. 1994, ApJ, 431, L75
Mathur, S., Wilkes, B., Elvis, M., & Fiore, F. 1994, ApJ, 434, 493
McDowell, J. C., Elvis, M., Wilkes, B. J., Willner, S. P., Oey, M. S., Polomski, E., Bechtold, J., & Green, R. F. 1989, ApJ, 345, L13
Nandy, K., Morgan, D. H., Willis, A. J., Wilson, R., & Gondhalekar, P. M. 1981, MNRAS, 196, 955
Netzer, H., & Laor, A. 1993, ApJ, 404, L51
Neugebauer, G., Green, R. F., Matthews, K., Schmidt, M., Soifer, B. T., & Bennett, J. 1987, ApJS, 63, 615
Neugebauer, G., Oke, J. B., Becklin, E. E., & Matthews, K. 1979, ApJ, 230, 79
Neugebauer, G., Soifer, B. T., Matthews, K., & Elias, J. H. 1989, AJ, 97, 957
Neugebauer, G., Soifer, B. T., Matthews, K., Margon, B., & Chanan, G. A. 1982, AJ, 87, 1639
Orr, J. B., & Browne, I. W. A. 1982, MNRAS, 200, 1067
Osterbrock, D. E. 1989, Astrophysics of Gaseous Nebulae and Active Galactic Nuclei (Mill Valley, CA: Univ. Sci.)
Ostriker, J. P., & Heisler, J. 1984, ApJ, 278, 1
Pei, Y. C., & Fall, S. M. 1995, ApJ, 454, 69
Pei, Y. C., Fall, S. M., & Bechtold, J. 1991, ApJ, 378, 6
Persic, M., & Salucci, P. 1992, MNRAS, 258, 14P
Pervot, M. L., Lequeux, J., Maurice, E., Pervot, L., & Rocca-Volmerange, B. 1984, A&A, 132, 389
Pettini, M., Smith, L. J., Hunstead, R. W., & King, D. L. 1994, ApJ, 426, 79
Rao, S., & Briggs, F. H. 1993, ApJ, 419, 515
Savage, B. D., & Mathis, J. S. 1979, ARA&A, 17, 73
Schmidt, M., & Green, R. F. 1983, ApJ, 269, 352
Serjeant, S., & Rawlings, S. 1996, Nature, 379, 304
Soifer, B. T., Neugebauer, G., Oke, J. B., Matthews, K., & Lacy, J. H. 1983, ApJ, 265, 18
Sprayberry, D., & Foltz, C. G. 1992, ApJ, 390, 39
Steidel, C. C. 1990, ApJS, 74, 37
Steidel, C. C., & Sargent, W. L. W. 1991, ApJ, 382, 433
———. 1992, ApJS, 80, 1
Srianand, R., & Khare, P. 1994, ApJ, 428, 82
———. 1996, MNRAS, 280, 767
Webster, R., Francis, P. J., Peterson, B. A., Drinkwater, M. J., & Masci, F. J. 1995, Nature, 375, 469
Wills, B. J., & Browne, I. W. A. 1986, MNRAS, 302, 56
Wills, B. J., Netzer, H., Brotherton, M. S., Han, M., Wills, D., Baldwin, J. A., Ferland, G. J., & Browne, I. W. A. 1993, ApJ, 410, 534
Wills, B. J., Wills, D., Breger, M., Antonucci, R. R. J., & Barvainis, R. 1992, ApJ, 398, 454
Wolfe, A. M., Lanzetta, K. M., Foltz, C. B., & Chaffee, F. H. 1995, ApJ, 454, 698
Wright, E. L. 1986, ApJ, 311, 156
Wright, E. L., Ables, J. G., & Allen, D. A. 1983, MNRAS, 205, 793
Zombeck, M. V. 1990, Handbook of Space Astronomy and Astrophysics (2d ed.; Cambridge: Cambridge Univ. Press)